Published in final edited form as:
Langmuir. 2012 December 4; 28(48): 16596–16604. doi:10.1021/la3025364.

Differential Effects of the Hydrophobic Surfactant Proteins on the Formation of Inverse Bicontinuous Cubic Phases

Mariya Chavarha[*], **Ryan W. Loney**[*], **Kamlesh Kumar**[*], **Shankar B. Rananavare**[†], and **Stephen B. Hall**[*,‡]

[*]Departments of Biochemistry & Molecular Biology, Medicine, and Physiology & Pharmacology, Oregon Health & Science University, Portland, OR 97239-3098

[†]Department of Chemistry, Portland State University, Portland, OR 97207

Abstract

Prior studies have shown that the biological mixture of the two hydrophobic surfactant proteins, SP–B and SP–C, produces faster adsorption of the surfactant lipids to an air/water interface, and that they induce 1-palmitoyl-2-oleoyl phosphatidylethanolamine (POPE) to form inverse bicontinuous cubic phases. Previous studies have shown that SP–B has a much greater effect than SP–C on adsorption. If the two proteins induce faster adsorption and formation of the bicontinuous structures by similar mechanisms, then they should also have different abilities to form the cubic phases. To test this hypothesis, we measured small angle X-ray scattering on the individual proteins combined with POPE. SP–B replicated the dose-related ability of the combined proteins to induce the cubic phases at temperatures more than 25°C below the point at which POPE alone forms the curved inverse-hexagonal phase. With SP–C, diffraction from cubic structures was either absent or present at very low intensities only with larger amounts of protein. The correlation between the structural effects of inducing curved structures and the functional effects on the rate of adsorption fits with the model in which SP–B promotes adsorption by facilitating formation of an inversely curved, rate-limiting structure.

Keywords

adsorption; bending; curvature; lipid polymorphisms; lung; pulmonary surfactant

INTRODUCTION

In the alveolar air sacks of the lungs, the type II pneumocytes synthesize and secrete a mixture of lipids[1] and proteins that acts as a surfactant. The material adsorbs to the air/water interface of the liquid layer that covers the alveolar surface and forms a thin film that lowers surface tension. Adsorption happens quickly. During either inflation with air of a fully deflated, excised lung[2] or the first few breaths of a newborn animal,[3] the recoil pressures required to counteract surface tension stabilize within minutes,[2] if not seconds,[3] indicating the rapid completion of adsorption. Studies in vitro show that the hydrophobic surfactant proteins (SPs), SP–B and SP–C, greatly increase the rate at which the surfactant lipids adsorb. With a clean interface, devoid of a film, the high surface tension can drive adsorption of vesicles containing only lipids.[4] Approaching the equilibrium spreading tension, adsorption requires the proteins.[4]

[‡]To whom correspondence should be addressed: Stephen B. Hall, Pulmonary & Critical Care Medicine, Mail Code UHN-67, Oregon Health & Science University, Portland, Oregon 97239-3098, Telephone: (503) 494-6667, sbh@ohsu.edu.

Any model of how the proteins promote adsorption must explain a fundamental observation. The proteins accelerate adsorption whether restricted to the vesicles or to preexisting films at the interface.[5, 6] These findings suggest that the proteins affect a rate-limiting structure that is accessible from both locations. An hourglass-shaped stalk extending between the adsorbing vesicles and the air/water interface[7, 8] (Fig. 1), analogous to the stalk proposed as an intermediate in the fusion of two vesicles,[9] would fit these requirements. The proteins would promote adsorption by facilitating formation of that structure.

Curvature represents a prominent feature of the proposed intermediate. Several factors known to alter the curvature of lipid leaflets also affect the adsorption of lipid vesicles. The phosphatidylethanolamines (PEs) form the inverse hexagonal (H_{II}) phase, in which the hydrophilic surface of the cylindrical monolayers is concave, indicating negative curvature. Gramicidin A enhances the negative net, or geometric, curvature of lipids in the H_{II} phase.[10] Both PE and gramicidin A increase rates of adsorption.[6, 11–13] Lysophosphatidylcholine, which forms positively curved micelles, instead inhibits adsorption.[13] These results suggest that negative curvature is a kinetically important characteristic of the rate-limiting intermediate. They also suggest that the SPs might accelerate adsorption by promoting curvature.

Determining whether the proteins affect curvature has been difficult. The surfactant lipids, with or without the SPs, form lamellar bilayers. The leaflets in these structures may have significant spontaneous curvature despite their planar configuration. Lipid leaflets with spontaneous curvature form structures that reflect a pair of free energies which can not be minimized simultaneously.[14, 15] In contrast to planar bilayers, curved structures minimize the energy of bending the leaflets away from their spontaneous curvature, but at the cost of stretching some acyl chains from their lowest energy extension to fill unoccupied space.[14, 15] Planar bilayers instead optimize the packing of chains, but at the cost of bending-energy.[14, 15] If chain-packing dominates, the leaflets form planar bilayers, despite the spontaneous curvature.[14, 15] Lipid-protein mixtures that form lamellar bilayers therefore can provide no evidence either for or against an effect of the proteins on curvature.

The effects of constituents on curvature depend on the effective molecular shape,[16–18] and are generally considered additive.[e.g. 19–24] Consequently the contribution of the SPs toward spontaneous curvature should be similar with different sets of lipids. Leaflets with a more pronounced negative curvature shift the balance between chain-packing and bending, and might allow the expression of a tendency to curve. Recent studies show that as little as 0.03% (w:w) SPs convert 1-palmitoyl-2-oleoyl phosphatidylethanolamine (POPE) from lamellar bilayers to the continuously saddle-shaped structures of the inverse cubic phases (Q_{II}).[25] Along with suggestive results from nuclear magnetic resonance,[26–28] these findings provide direct support that the SPs can affect the curvature of lipid leaflets.

The studies reported here concern the effects of the individual proteins, SP–B and SP–C. Previous reports have shown that although both proteins promote adsorption, SP–B is much more effective than SP–C.[29] This difference may well explain why the absence of SP-B is promptly fatal at birth,[30, 31] but patients without SP-C usually survive to develop interstitial lung disease later in life.[31–33] If the proteins induce faster adsorption and formation of the Q_{II} phases by similar mechanisms, then the structural effects of the combined proteins should originate mostly from SP–B. These studies tested that hypothesis by using small angle X-ray scattering (SAXS) to determine how the individual proteins affect the structures formed by POPE.

MATERIALS AND METHODS

Materials

POPE was purchased from Avanti Polar Lipids (Alabaster, AL) and used without further characterization or purification. All reagents and solvents were ACS grade and obtained commercially from the following sources: NaCl, $CaCl_2$, chloroform and methanol (Mallinckrodt, Hazelwood, MO); UltraPure™ $Na_2EDTA\text{-}2H_2O$ (Invitrogen, Grand Island, NY); NaN_3 (Fluka Biochemika, Buchs, Switzerland); 4-(2-hydroxyethyl)-1-piperazineethanesulfonic acid (HEPES) (Sigma, St. Louis, MO). Water was processed and photo-oxidized with ultraviolet light using a NANOpure Diamond TOC-UV water-purification system (Barnstead / Thermolyne, Dubuque, IA). Extracted calf surfactant (calf lung surfactant extract, CLSE), provided by Dr. Edmund Egan (ONY, Inc., Amherst, NY), was obtained by lavaging calf lungs, recovering the surfactant aggregates by centrifugation, and extracting the hydrophobic constituents from the pelleted material.[34]

Methods

Separation of the surfactant proteins—The combined hydrophobic proteins were obtained from CLSE by gel permeation chromatography with a matrix of LH-20,[35] using a solvent of chloroform:methanol (1:1, v:v).[36] SP–B was separated from the combined proteins by licensed use of a patented procedure[37, 38] based on the preferential partitioning of SP–B and SP–C into different phases formed by chloroform-methanol-water.[39] The upper methanol-rich layer contained pure SP–B, which was dried by rotary evaporation and resuspended in chloroform-methanol (1:1, v:v). The lower chloroform-rich layer contained both proteins, which were separated by gel permeation chromatography on a matrix of LH-60[40, 41] to yield the purified SP–C. Samples were eluted with a mobile phase of chloroform:methanol (1:1, v:v) driven by gravity and monitored by optical density at 240 and 280 nm.[42] The extent of the different proteins in different fractions was determined by staining of proteins separated electrophoretically on polyacrylamide gels.

Biochemical characterization—The content of phospholipid was determined by measuring the amount of phosphate present.[43] Total protein was determined with amido black on material precipitated by trichloroacetic acid.[44] The molecular weights of separated proteins were established by electrophoresis on polyacrylamide gels containing sodium dodecyl sulphate (NuPAGE®, Invitrogen, Carlsbad, CA). Reduced samples used dithiothreitol at a final concentration of 50 mM. Proteins suspended in buffered lithium dodecyl sulfate were incubated at 70°C for 15 min, loaded on 4–12% gradient Bis/Tris gels, and run at a constant voltage of 200 V. The proteins were detected by incubation overnight with SYPRO® Ruby stain (Invitrogen, Carlsbad, CA).

Preparation of vesicles—The proteins were combined with the lipids in mixtures of chloroform and methanol, the ratio of which varied with the content of protein. Solvent was evaporated initially under a stream of nitrogen followed by incubation overnight at 2 mbar. The lipid-protein mixtures were dispersed in 2 mM EDTA with 0.002% (w:w) NaN_3 to a final concentration of 50 mM phospholipid by hydrating overnight at 4°C followed by vigorous vortexing and cyclic freezing and thawing. The samples were transferred to capillaries (1.0 mm diameter, 0.01 mm wall thickness; "special glass"; Charles Supper, Natick, MA), centrifuged at 640 × g_{max} for 10 min, sealed with flame and epoxy, and stored at 4°C until use.

Small angle x-ray scattering—Diffraction was measured on beamline 1–4 at the Stanford Synchrotron Radiation Lightsource (SSRL). Up to 20 capillaries were mounted on an aluminum block, the temperature of which was controlled with water pumped from a

circulating bath and monitored with an externally applied thermocouple. Block-temperatures were converted to sample-temperatures according to relationships established by melting a series of compounds with known melting points. Samples were equilibrated for at least 10 minutes at each temperature before exposure to radiation with a wavelength of 1.488 Å for 120 seconds. Angular dependence was calibrated using standard samples of silver behenate, cholesterol myristate, and lead stearate. The rings produced by powder diffraction were radially integrated using the program Fit2D[45] to obtain plots of intensity versus the scattering vector (q). Lamellar, hexagonal, and cubic space groups were assigned according to the best fit of the measured values of q for the diffraction peaks to the Miller indices allowed for the different structures.[25, 46] The slopes of the linear relationship between measured q and allowed values of $\sqrt{l^2+m^2+n^2}$ provided the lattice-constants (a_o) of the unit cells according to ($a_o = 2\pi/\text{slope}$) for the lamellar and cubic phases, and ($a_o = 4\pi/(\sqrt{3} \cdot \text{slope})$) for the hexagonal phase.

The results presented here were obtained using a single set of samples. Measurements with samples containing the same preparation of protein (SP–B; SP–C; or the combined proteins) were made at the same sequential temperatures. Three distinct sets of samples, with some measurements on beamline 4–2, produced comparable results, although in one case, samples with 0.3 and 1.0% SP–C did produce minor peaks with Q_{II} spacing. Intensities in that case were well below the levels for samples with the combined proteins and with SP–B. Resuspension of the lipid-protein mixtures in buffered electrolyte (150 mM NaCl, 1.5 mM $CaCl_2$, 10 mM HEPES pH 7.0) rather than EDTA produced no effect on the results.

Calculation of average curvature for bicontinuous cubic phases—The average magnitude of the principal curvatures, $\langle|c|\rangle$, was obtained using previously derived relationships.[47, 48] Because the midpoint of the bilayer in the bicontinuous cubic phases follows a minimal surface, net curvature (c_1+c_2) for the bilayer is uniformly zero, and the principal curvatures are always equal in magnitude and opposite in sign, $c_1 = -c_2$. The Gaussian curvature, $K = c_1 \cdot c_2$, varies throughout the structure, but the average magnitude, $\langle|K|\rangle$, and the similar average of the principal curvatures, $\langle|c|\rangle$, can be calculated from a homogeneity index, H, that expresses the variation of K for the particular surface according to

$$\langle|c|\rangle = \langle|K|\rangle^{1/2} = \frac{1}{a_o} \cdot \left(\frac{-2\pi\chi}{H}\right)^{1/3}$$

where χ is the Euler characteristic.[47, 48] The previously determined values of (χ, H) for the Q_{II} phases with space-groups $Pn\bar{3}m$ and $Im\bar{3}m$, (−2, 0.750) and (−4, 0.716), respectively,[48] allowed calculation of $\langle|c|\rangle$ for the cubic phases formed by the different preparations.

RESULTS

Our samples used proteins obtained by a previously described[37, 38] but unused protocol. After separation of the proteins from the surfactant lipids by established chromatographic methods,[35, 36, 41] the two proteins were separated from each other using a licensed protocol based on differential extraction.[37, 38] Omission of acid from all solvents at all steps of the protocol minimized the possibility that the proteins would be modified. Electrophoresis on gradient gels showed molecular weights of roughly 21 and 8 kDa for the unreduced and reduced samples of SP–B, respectively (Fig. 2). These mobilities were consistent with results obtained previously for purified SP–B,[42, 49] which forms a crosslinked dimer of two 79-amino acid peptides. Samples of monomeric SP–C (35 amino acids) produced a band at

approximately 7 kDa that was unchanged by a reducing agent (Fig. 2), consistent with the expected behavior of that monomeric peptide.[50] The gels showed minimal cross-contamination of the purified samples by the other protein (Fig. 2).

Measurements of SAXS for POPE alone and with the combined proteins produced expected results. POPE by itself converted from one lamellar spacing to another between 21 and 30°C, and to a hexagonal phase beginning at 70°C (Fig. 3A,4). These results were consistent with the calorimetrically determined transitions from $L_{\beta'}$ to L_{α} phases at 26°C,[51] and from L_{α} to H_{II} at 71°C.[52] The combined proteins induced diffraction at intervals expected from cubic space groups (Fig. 3A,4A). In samples containing 0.01% SP, diffraction consistent with $Pn\bar{3}m$ structures began at 61°C; $Im\bar{3}m$ spacing emerged at 70°C (Fig. 3A,4A). Increasing amounts of protein lowered the temperature at which the cubic phases first appeared, reaching 30°C at 5% SP (Fig. 4A). The hexagonal phase, which coexisted with the Q_{II} phases in samples containing small amounts of protein, was absent above 0.03% SP (Fig. 4A). In these respects, our findings here confirmed the results reported previously for the combined proteins with POPE.[25]

The one aspect of our current findings that had not been evident from our prior results was a dose-dependent decrease in the Q_{II} lattice constant (Fig. 4). This change was most evident when expressed in terms of the average magnitude of the bilayer curvatures obtained from the average magnitude of the Gaussian curvature, $\langle|c|\rangle = \langle|K|\rangle^{1/2}$. The increase in curvature produced by the proteins occurred with both Q_{II} phases, and was not subtle. Between 0.01 and 5.0% SP, the increase in $\langle|c|\rangle$ reached 23% (Fig. 5). This increase occurred predominantly with smaller amounts of protein. With the $Pn\bar{3}m$ phase at 61°C, for instance, over two-thirds of the change between 0.01 and 5.0% SP occurred at ≤ 0.1% SP.

SP–B alone replicated the effects of the combined proteins. Like the mixed SPs, SP–B produced no change in either the transition-temperatures of the lamellar phases or their lattice-constants. Small amounts of SP–B, similar to the levels of the combined proteins that achieved the same effect, induced the formation of the Q_{II} phases (Fig. 3–4). Diffraction for both $Pn\bar{3}m$ and $Im\bar{3}m$ space groups appeared with as little as 0.03% SP–B (Figs. 3–4). Like the combined proteins, greater amounts of SP–B lowered the temperature at which the Q_{II} phases appeared, reaching 43°C for the $Im\bar{3}m$ space group at 5.0% SP–B. The dose-dependent increase in curvature produced by the combined proteins also occurred with SP-B alone (Fig. 5B,D). Comparison of the curvatures for the two sets of samples showed that with both Q_{II} phases, the effects of SP-B fully explained the changes produced by the combined proteins.

In contrast to SP-B, SP–C produced little change in the behavior of the lipids. The protein in concentrations from 0.01 – 1.0% had no effect on the transition-temperatures or the lattice-constant for the lamellar or the H_{II} phases. SP–C either failed to produce any evidence of the Q_{II} phases (Fig. 3,4), or, with other preparations not shown here, produced only traces of Q_{II} diffraction with samples containing 0.3 or 1.0% SP-C. For a single preparation, the hexagonal lattice-constant at 3% SP–C also decreased from the value with lower amounts of protein, but for the other samples, the value remained invariant. Any ability of SP–C to alter the structure of the lipids, if present, was greatly reduced relative to SP–B.

DISCUSSION

The studies reported here provide a simple test of a model for how the hydrophobic surfactant proteins promote adsorption. The model predicts that the proteins facilitate formation of an hourglass-shaped stalk that connects the adsorbing vesicle to the air/water interface (Fig. 1). Consistent with the model, low amounts of the combined proteins convert

POPE from lamellar structures to Q_{II} phases,[25] in which each leaflet has the negative net and Gaussian curvatures predicted for the rate-limiting kinetic intermediate (Fig. 1). The efficiencies with which the individual proteins promote adsorption are different.[29] If induction of the Q_{II} phases reflects the same mechanisms that lead to faster adsorption, then the two proteins should have different abilities to generate the Q_{II} structures.

Our results confirm that hypothesis. In the same low amounts as the combined proteins, SP–B induces formation of the Q_{II} phases. SP–C, which has a much smaller effect on adsorption,[29] either fails at all levels to generate Q_{II} diffraction or induces only low intensity peaks with higher levels of the protein. Our results indicate that, like adsorption, the induction by the combined proteins of the Q_{II} phases reflects primarily the effects of SP–B. These findings establish the predicted correlation between the structural and functional effects of the two proteins.

The model contends that SP–B induces both POPE and the surfactant lipids to adopt curvature by a similar mechanism. The processes could be either thermodynamic or kinetic. A kinetic effect would require that, under the conditions at which SP–B induces the Q_{II} phases, lamellar POPE would be metastable. The proteins would induce the structural changes by reducing a kinetic barrier that limits access to the Q_{II} phases rather than by stabilizing them. The behavior of lipids that form curved structures supports that possibility. Although lipids generally convert during heating directly from the L_α to H_{II} phase, repeated cycling through the L_α-H_{II} transition can induce the Q_{II} structures.[53] These findings suggest that over a range of temperatures, the Q_{II} phases may represent the most stable structures, but that they are kinetically inaccessible. According to this kinetic model, SP–B would induce the Q_{II} phases and promote faster adsorption by providing a lower-energy pathway to the curved structures.

The proteins could also produce a thermodynamic stabilization of the curved structures, whether the bicontinuous cubic phases or the hypothetical kinetic intermediate in adsorption, by several specific mechanisms. The free energy of the structures that determine their relative stabilities includes contributions from bending, the stretching of acyl chains, and interactions between adjacent bilayers.[54, 55] SP-B seems most likely to change the energy of bending. The protein produces no shift in the spacing of the lamellar bilayers (Fig. 4), arguing against a change in the interaction between adjacent bilayers. The energy of stretched chains is small in Q_{II} bilayers,[56, 57] arguing that neither SP-B nor any other factor is likely to induce the lamellar-to-Q_{II} transition by changing chain-packing. The dose-dependent change in Q_{II}-curvature (Fig. 5) instead favors an effect of SP-B on the energy of bending.

The components of bending energy, including the spontaneous curvature of the leaflets and their flexibilities of simple-splay and saddle-splay curvature, all originate in the lateral stress profile of the monolayer.[58–64] SP-B could affect any or all of these components. Perhaps the most important point, however, is that SP-B should produce comparable shifts in the stress profile of different lipids. The mechanism by which SP-B induces POPE to form the Q_{II} phase should also favor the formation of the hypothetical kinetic intermediate (Fig. 1) by the surfactant lipids.

Our results with the individual SPs agree with the behavior of other lipid-protein mixtures. Most peptides that induce Q_{II} phases form amphipathic helices[65–70]. SP-B consists of a crosslinked pair of 79-amino acid peptides, the sequence of which suggests a series of amphipathic helices.[71] Although proposals concerning how the two monomeric peptides fit together in the dimer have been conspicuously absent,[72] vibrational spectroscopy supports the extent of secondary structure suggested by the sequence.[73] The primary structure of SP–

C instead would generate a single hydrophobic helix.[50] The structure of the proteins that induce Q_{II} phases therefore predicts the differential effect of the individual SPs.

Our results also fit with the general relationship between fusion and the Q_{II} phases. The processes of interfacial adsorption and fusion of two bilayers are energetically distinct, with adsorption driven by the reduction in surface tension that is absent from fusion. Both processes, however, involve the transformation of stable bilayers into new structures along a pathway that must involve transiently greater exposure of hydrophobic groups to the aqueous environment. The hypothetical intermediate in adsorption is also structurally analogous to the stalk proposed to form from the outer leaflets of two fusing vesicles. The intermediates proposed for both processes prominently feature leaflets with negative curvature. Fusion proceeds more readily under conditions that favor formation of the Q_{II} phases.[74] Those results and the ability of SP-B to induce Q_{II} phases support the possibility that SP-B promotes adsorption by facilitating formation of an inversely curved, rate-limiting structure.

Our results are subject to a final reservation. The correlation between the induction of the Q_{II} phases and promotion of faster adsorption supports the importance of curvature in determining the rate of adsorption. The model of the bridging stalk nicely explains both the role of curvature and the effect of constituents in preexisting films. Other models,[75] however, remain possible.

In summary, SP–B, but not SP–C, replicates the ability of the combined proteins to induce POPE to form Q_{II} phases more than 25°C below the L_{α}-H_{II} transition for the lipid alone. These results fit with a model that explains the much greater ability of SP–B than SP–C to promote faster adsorption in terms of effects on a rate-limiting structure in which lipid leaflets have negative net and Gaussian curvatures.

Acknowledgments

These studies were supported by funds from the National Institutes of Health (HL 54209). CLSE was provided by Dr. Edmund Egan (ONY, Inc., Amherst, NY). The procedure for purifying SP–B and SP–C was based on a patented protocol under license from ONY, Inc. Measurements of SAXS were performed at the Stanford Synchrotron Radiation Lightsource, a national user-facility operated by Stanford University on behalf of the U.S. Department of Energy, Office of Basic Energy Sciences. The authors thank Leonard E. Schulwitz Jr. and Hamed Khoojinian for assistance in conducting and analyzing measurements that contributed to these studies.

REFERENCES

1. Postle AD, Heeley EL, Wilton DC. A comparison of the molecular species compositions of mammalian lung surfactant phospholipids. Comp. Biochem. Physiol. A Mol. Integr. Physiol. 2001; 129(1):65–73. [PubMed: 11369534]
2. Clements JA. Functions of the alveolar lining. Am. Rev. Respir. Dis. 1977; 115(6 part 2, 6 part 2): 67–71. [PubMed: 577382]
3. Lachmann B, Grossmann G, Nilsson R, Robertson B. Lung mechanics during spontaneous ventilation in premature and fullterm rabbit neonates. Respir. Physiol. 1979; 38(3):283–302. [PubMed: 523846]
4. Loney RW, Anyan WR, Biswas SC, Rananavare SB, Hall SB. The accelerated late adsorption of pulmonary surfactant. Langmuir. 2011; 27(8):4857–4866. [PubMed: 21417351]
5. Oosterlaken-Dijksterhuis MA, Haagsman HP, van Golde LMG, Demel RA. Interaction of lipid vesicles with monomolecular layers containing lung surfactant proteins SP-B or SP-C. Biochemistry. 1991; 30(33):8276–8281. [PubMed: 1868098]
6. Biswas SC, Rananavare SB, Hall SB. Effects of gramicidin-A on the adsorption of phospholipids to the air-water interface. Biochim. Biophys. Acta. 2005; 1717(1):41–49. [PubMed: 16242116]

7. Walters RW, Jenq RR, Hall SB. Distinct steps in the adsorption of pulmonary surfactant to an air-liquid interface. Biophys. J. 2000; 78(1):257–266. [PubMed: 10620290]

8. Klenz U, Saleem M, Meyer MC, Galla HJ. Influence of lipid saturation grade and headgroup charge: a refined lung surfactant adsorption model. Biophys. J. 2008; 95(2):699–709. [PubMed: 18390619]

9. Markin VS, Kozlov MM, Borovjagin VL. On the theory of membrane fusion. The stalk mechanism. Gen. Physiol. Biophys. 1984; 3(5):361–377. [PubMed: 6510702]

10. Szule JA, Rand RP. The effects of gramicidin on the structure of phospholipid assemblies. Biophys. J. 2003; 85(3):1702–1712. [PubMed: 12944285]

11. Yu S-H, Harding PGR, Possmayer F. Artificial pulmonary surfactant. Potential role for hexagonal H_{II} phase in the formation of a surface-active monolayer. Biochim. Biophys. Acta. 1984; 776:37–47.

12. Perkins WR, Dause RB, Parente RA, Minchey SR, Neuman KC, Gruner SM, Taraschi TF, Janoff AS. Role of lipid polymorphism in pulmonary surfactant. Science. 1996; 273(5273):330–332. [PubMed: 8662513]

13. Biswas SC, Rananavare SB, Hall SB. Differential effects of lysophosphatidylcholine on the adsorption of phospholipids to an air/water interface. Biophys. J. 2007; 92(2):493–501. [PubMed: 17056729]

14. Charvolin J, Sadoc JF. Periodic systems of frustrated fluid films and <<bicontinuous>> cubic structures in liquid crystals. J. Phys. (Paris). 1987; 48(9):1559–1569.

15. Gruner SM. Stability of lyotropic phases with curved interfaces. J. Phys. Chem. 1989; 93:7562–7570.

16. Tartar HV. A theory of the structure of the micelles of normal paraffin-chain salts in aqueous solution. J. Phys. Chem. 1955; 59(12):1195–1199.

17. Tanford, C. The Hydrophobic Effect: Formation of Micelles and Biological Membranes. 1 ed. New York: Wiley; 1973. p. 200

18. Israelachvili JN, Marcelja S, Horn RG. Physical principles of membrane organization. Q. Rev. Biophys. 1980; 13(2):121–200. [PubMed: 7015403]

19. Kirk GL, Gruner SM. Lyotropic effects of alkanes and headgroup composition on the L_{α}-H_{II} lipid liquid crystal phase transition: hydrocarbon packing versus intrinsic curvature. J. Phys. (Paris). 1985; 46(5):761–769.

20. Tate MW, Gruner SM. Lipid polymorphism of mixtures of dioleoylphosphatidylethanolamine and saturated and monounsaturated phosphatidylcholines of various chain lengths. Biochemistry. 1987; 26(1):231–236. [PubMed: 3828299]

21. Rand RP, Fuller NL, Gruner SM, Parsegian VA. Membrane curvature, lipid segregation, and structural transitions for phospholipids under dual-solvent stress. Biochemistry. 1990; 29(1):76–87. [PubMed: 2322550]

22. Chen Z, Rand RP. The influence of cholesterol on phospholipid membrane curvature and bending elasticity. Biophys. J. 1997; 73(1):267–276. [PubMed: 9199791]

23. Szule JA, Fuller NL, Rand RP. The effects of acyl chain length and saturation of diacylglycerols and phosphatidylcholines on membrane monolayer curvature. Biophys. J. 2002; 83(2):977–984. [PubMed: 12124279]

24. Kooijman EE, Chupin V, Fuller NL, Kozlov MM, de Kruijff B, Burger KNJ, Rand PR. Spontaneous curvature of phosphatidic acid and lysophosphatidic acid. Biochemistry. 2005; 44(6): 2097–2102. [PubMed: 15697235]

25. Chavarha M, Khoojinian H, Schulwitz LE Jr, Biswas SC, Rananavare SB, Hall SB. Hydrophobic surfactant proteins induce a phosphatidylethanolamine to form cubic phases. Biophys. J. 2010; 98(8):1549–1557. [PubMed: 20409474]

26. Dico AS, Hancock J, Morrow MR, Stewart J, Harris S, Keough KMW. Pulmonary surfactant protein SP-B interacts similarly with dipalmitoylphosphatidylglycerol and dipalmitoylphosphatidylcholine in phosphatidylcholine/phosphatidylglycerol mixtures. Biochemistry. 1997; 36(14):4172–4177. [PubMed: 9100011]

27. Morrow MR, Stewart J, Taneva S, Dico A, Keough KM. Perturbation of DPPC bilayers by high concentrations of pulmonary surfactant protein SP-B. Eur. Biophys. J. 2004; 33(4):285–290. [PubMed: 14504839]
28. Farver RS, Mills FD, Antharam VC, Chebukati JN, Fanucci GE, Long JR. Lipid polymorphism induced by surfactant peptide SP-B(1-25). Biophys. J. 2010; 99(6):1773–1782. [PubMed: 20858421]
29. Wang Z, Gurel O, Baatz JE, Notter RH. Differential activity and lack of synergy of lung surfactant proteins SP-B and SP-C in interactions with phospholipids. J. Lipid Res. 1996; 37(8):1749–1760. [PubMed: 8864959]
30. Nogee LM, de Mello DE, Dehner LP, Colten HR. Brief report: deficiency of pulmonary surfactant protein B in congenital alveolar proteinosis. New Engl. J. Med. 1993; 328(6):406–410. [PubMed: 8421459]
31. Nogee LM. Alterations in SP-B and SP-C expression in neonatal lung disease. Annu. Rev. Physiol. 2004; 66:601–623. [PubMed: 14977415]
32. Nogee LM, Dunbar AE 3rd, Wert SE, Askin F, Hamvas A, Whitsett JA. A mutation in the surfactant protein C gene associated with familial interstitial lung disease. New Engl. J. Med. 2001; 344(8):573–579. [PubMed: 11207353]
33. Lawson WE, Grant SW, Ambrosini V, Womble KE, Dawson EP, Lane KB, Markin C, Renzoni E, Lympany P, Thomas AQ, Roldan J, Scott TA, Blackwell TS, Phillips JA 3rd, Loyd JE, du Bois RM. Genetic mutations in surfactant protein C are a rare cause of sporadic cases of IPF. Thorax. 2004; 59(11):977–980. [PubMed: 15516475]
34. Notter RH, Finkelstein JN, Taubold RD. Comparative adsorption of natural lung surfactant, extracted phospholipids, and artificial phospholipid mixtures to the air-water interface. Chem. Phys. Lipids. 1983; 33(1):67–80. [PubMed: 6688762]
35. Takahashi A, Fujiwara T. Proteolipid in bovine lung surfactant: its role in surfactant function. Biochem. Biophys. Res. Comm. 1986; 135(2):527–532. [PubMed: 3754441]
36. Hall SB, Wang Z, Notter RH. Separation of subfractions of the hydrophobic components of calf lung surfactant. J. Lipid Res. 1994; 35(8):1386–1394. [PubMed: 7989863]
37. Egan EA, Hlavaty LM, Holm BA. Compositions and methods for isolating lung surfactant hydrophobic proteins SP-B and SP-C. 6,020,307. 2000
38. Egan EA, Hlavaty LM, Holm BA. Compositions and methods for isolating lung surfactant hydrophobic proteins SP-B and SP-C. 6,458,759. 2002
39. Bligh E, Dyer W. A rapid method of total lipid extraction and purification. Can. J. Biochem. 1959; 37:911–917. [PubMed: 13671378]
40. Warr RG, Hawgood S, Buckley DI, Crisp TM, Schilling J, Benson BJ, Ballard PL, Clements JA, White RT. Low molecular weight human pulmonary surfactant protein (SP5): isolation, characterization, and cDNA and amino acid sequences. Proc. Natl. Acad. Sci. U.S.A. 1987; 84(22):7915–7919. [PubMed: 3479771]
41. Curstedt T, Jornvall H, Robertson B, Bergman T, Berggren P. Two hydrophobic low-molecular-mass protein fractions of pulmonary surfactant. Characterization and biophysical activity. Eur. J. Biochem. 1987; 168(2):255–262. [PubMed: 3665923]
42. Pérez-Gil J, Cruz A, Casals C. Solubility of hydrophobic surfactant proteins in organic solvent/water mixtures. Structural studies on SP-B and SP-C in aqueous organic solvents and lipids. Biochim. Biophys. Acta. 1993; 1168(3):261–270. [PubMed: 8323965]
43. Ames BN. Assay of inorganic phosphate, total phosphate and phosphatases. Meth. Enzymol. 1966; VIII:115–118.
44. Kaplan RS, Pedersen PL. Determination of microgram quantities of protein in the presence of milligram levels of lipid with amido black 10B. Anal. Biochem. 1985; 150(1):97–104. [PubMed: 4083487]
45. Hammersley AP, Svensson SO, Hanfland M, Fitch AN, Hausermann D. Two-dimensional detector software: From real detector to idealised image or two-theta scan. High Pressure Res. 1996; 14(4): 235–248.
46. Sun RG, Zhang J. The cubic phase of phosphatidylethanolamine film by small angle x-ray scattering. J. Phys. D: Appl. Phys. 2004; 37(3):463–467.

47. Hyde ST. Curvature and the global structure of interfaces in surfactant-water systems. J. Phys. Colloques. 1990; 51(C7):C7-209–C7-228.
48. Fogden A, Hyde ST. Continuous transformations of cubic minimal surfaces. Eur. Phys. J. B. 1999; 7(1):91–104.
49. Baatz JE, Zou Y, Cox JT, Wang ZD, Notter RH. High-yield purification of lung surfactant proteins SP-B and SP-C and the effects on surface activity. Protein Expr. Purif. 2001; 23(1):180–190. [PubMed: 11570861]
50. Johansson J, Curstedt T, Robertson B, Jörnvall H. Size and structure of the hydrophobic low molecular weight surfactant-associated polypeptide. Biochemistry. 1988; 27(10):3544–3547. [PubMed: 3408709]
51. Brown PM, Steers J, Hui SW, Yeagle PL, Silvius JR. Role of head group structure in the phase behavior of amino phospholipids. 2. Lamellar and nonlamellar phases of unsaturated phosphatidylethanolamine analogues. Biochemistry. 1986; 25(15):4259–4267. [PubMed: 3756138]
52. Epand RM, Bottega R. Modulation of the phase transition behavior of phosphatidylethanolamine by cholesterol and oxysterols. Biochemistry. 1987; 26(7):1820–1825. [PubMed: 3593694]
53. Shyamsunder E, Gruner SM, Tate MW, Turner DC, So PT, Tilcock CP. Observation of inverted cubic phase in hydrated dioleoylphosphatidylethanolamine membranes. Biochemistry. 1988; 27(7):2332–2336. [PubMed: 3382626]
54. Kirk GL, Gruner SM, Stein DL. A thermodynamic model of the lamellar to inverse hexagonal phase transition of lipid membrane-water systems. Biochemistry. 1984; 23(6):1093–1102.
55. Shearman GC, Ces O, Templer RH, Seddon JM. Inverse lyotropic phases of lipids and membrane curvature. J. Phys.-Condens. Mat. 2006; 18(28):S1105–S1124.
56. Anderson DM, Gruner SM, Leibler S. Geometrical aspects of the frustration in the cubic phases of lyotropic liquid crystals. Proc. Natl. Acad. Sci. U.S.A. 1988; 85(15):5364–5368. [PubMed: 3399497]
57. Templer RH, Seddon JM, Duesing PM, Winter R, Erbes J. Modeling the phase behavior of the inverse hexagonal and inverse bicontinuous cubic phases in 2-1 fatty acid/phosphatidylcholine mixtures. J. Phys. Chem. B. 1998; 102(37):7262–7271.
58. Harbich W, Servuss RM, Helfrich W. Passages in lecithin-water systems. Z. Naturforsch. 1978; 33a:1013–1017.
59. Petrov AG, Mitov MD, Derzhanski A. Saddle splay instability in lipid bilayers. Phys. Lett. A. 1978; 65(4):374–376.
60. Helfrich, W. Amphiphilic mesophases made of defects. In: Balian, R.; Kléman, M.; Poirier, J-P., editors. Physique des dÈfauts : les Houches, session XXXV, 28 Juillet–29 Ao°t 1980. North-Holland: Amsterdam; New York; Oxford: 1981. p. 716-755.
61. Helfrich, W.; Harbich, W. Equilibrium configurations of fluid membranes. In: Meunier, J.; Langevin, D.; Boccara, N., editors. Physics of Amphiphilic Layers : proceedings of the workshop; February 10–19, 1987; Les Houches, France. Berlin: Springer-Verlag; 1987. p. 58-63.
62. Helfrich, W. Elasticity and thermal undulations of fluid films of amphiphiles. In: Charvolin, J.; Joanny, JF.; Zinn-Justin, J., editors. Liquides aux Interfaces = Liquids at Interfaces. North-Holland: Amsterdam: 1990. p. 209-237.
63. Seddon JM. Structure of the inverted hexagonal (H_{II}) phase, and non-lamellar phase transitions of lipids. Biochim. Biophys. Acta. 1990; 1031(1):1–69. [PubMed: 2407291]
64. Helfrich W. Lyotropic lamellar phases. J. Phys.-Condens. Mat. 1994; 6(23A):A79–A92.
65. Angelova A, Ionov R, Koch MH, Rapp G. Interaction of the peptide antibiotic alamethicin with bilayer- and non-bilayer-forming lipids: influence of increasing alamethicin concentration on the lipids supramolecular structures. Arch. Biochem. Biophys. 2000; 378(1):93–106. [PubMed: 10871049]
66. Kamo T, Nakano M, Kuroda Y, Handa T. Effects of an amphipathic α-helical peptide on lateral pressure and water penetration in phosphatidylcholine and monoolein mixed membranes. J. Phys. Chem. B. 2006; 110(49):24987–24992. [PubMed: 17149920]

67. Hickel A, Danner-Pongratz S, Amenitsch H, Degovics G, Rappolt M, Lohner K, Pabst G. Influence of antimicrobial peptides on the formation of nonlamellar lipid mesophases. Biochim. Biophys. Acta. 2008; 1778(10):2325–2333. [PubMed: 18582435]

68. Zweytick D, Tumer S, Blondelle SE, Lohner K. Membrane curvature stress and antibacterial activity of lactoferricin derivatives. Biochem. Biophys. Res. Comm. 2008; 369(2):395–400. [PubMed: 18282464]

69. Fuhrmans M, Knecht V, Marrink SJ. A single bicontinuous cubic phase induced by fusion peptides. J. Am. Chem. Soc. 2009; 131(26):9166–9167. [PubMed: 19530654]

70. Keller SL, Gruner SM, Gawrisch K. Small concentrations of alamethicin induce a cubic phase in bulk phosphatidylethanolamine mixtures. Biochim. Biophys. Acta. 1996; 1278(2):241–246. [PubMed: 8593282]

71. Curstedt T, Johansson J, Barros-Soderling J, Robertson B, Nilsson G, Westberg M, Jornvall H. Low-molecular-mass surfactant protein type 1. The primary structure of a hydrophobic 8-kDa polypeptide with eight half-cystine residues. Eur. J. Biochem. 1988; 172(3):521–525. [PubMed: 3350011]

72. Whitsett JA, Weaver TE. Hydrophobic surfactant proteins in lung function and disease. New Engl. J. Med. 2002; 347(26):2141–2148. [PubMed: 12501227]

73. Vandenbussche G, Clercx A, Clercx M, Curstedt T, Johansson J, Jornvall H, Ruysschaert JM. Secondary structure and orientation of the surfactant protein SP-B in a lipid environment. Biochemistry. 1992; 31(38):9169–9176. [PubMed: 1390703]

74. Siegel, DP. The relationship between bicontinuous inverted cubic phases and membrane fusion. In. In: Lynch, ML.; Spicer, PT., editors. Bicontinuous Liquid Crystals. Boca Raton: Taylor & Francis; 2005. p. 59-98.

75. Kinnunen PK, Holopainen JM. Mechanisms of initiation of membrane fusion: role of lipids. Biosci Rep. 2000; 20(6):465–482. [PubMed: 11426689]

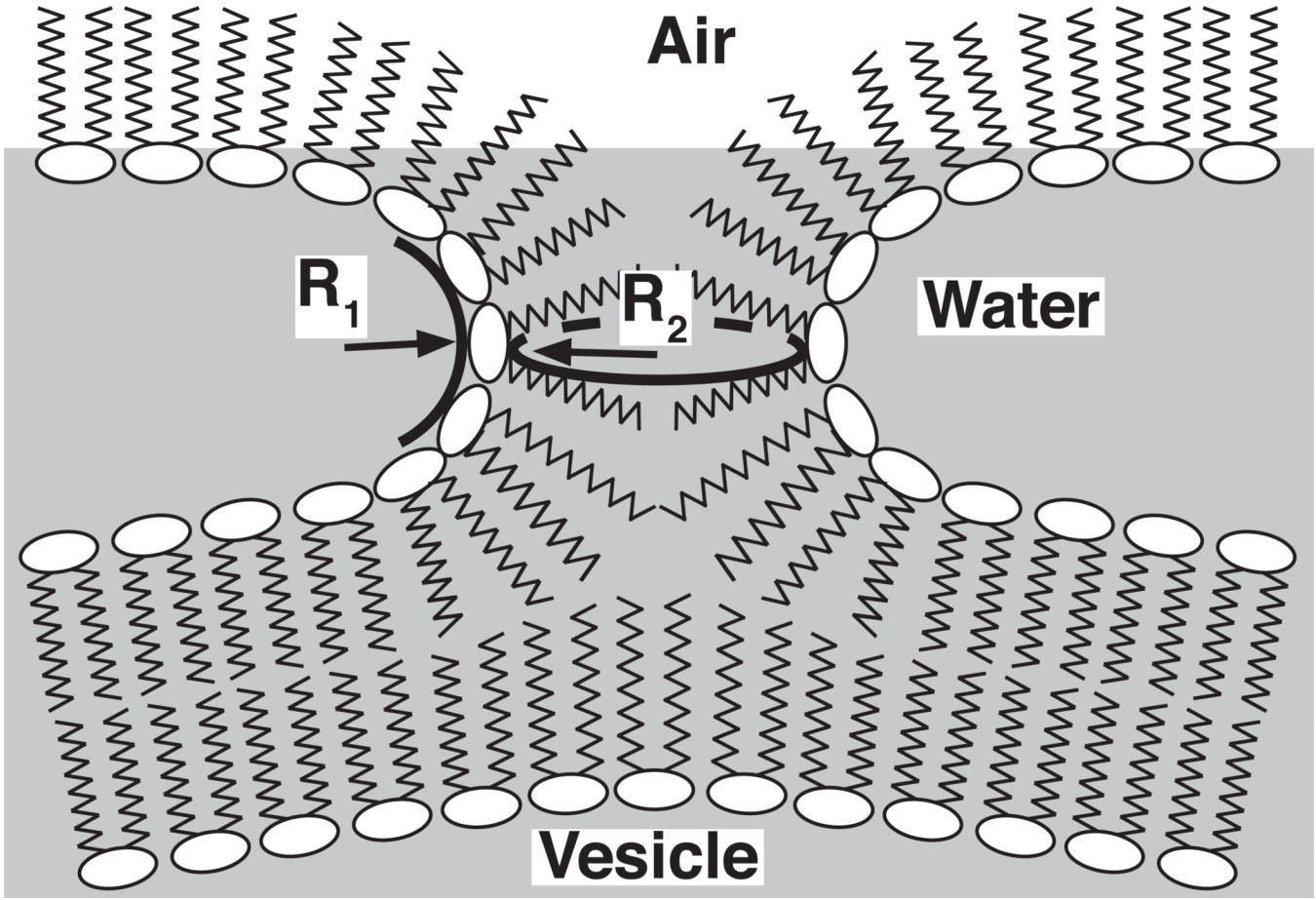

Figure 1.
Hypothetical structure of the kinetic intermediate that limits the rate of adsorption. The outer leaflet of the vesicle must invert to insert into the air/water interface with the correct orientation. The two principal curvatures of the intermediate structure would have opposite signs. In the plane perpendicular to the air/water interface, the curvature of the leaflet ($c_1 \equiv 1/R_1$), with its concave hydrophilic face, would by convention be negative. In the plane parallel to the interface, the curvature ($c_2 \equiv 1/R_2$) of the convex hydrophilic face would be positive.

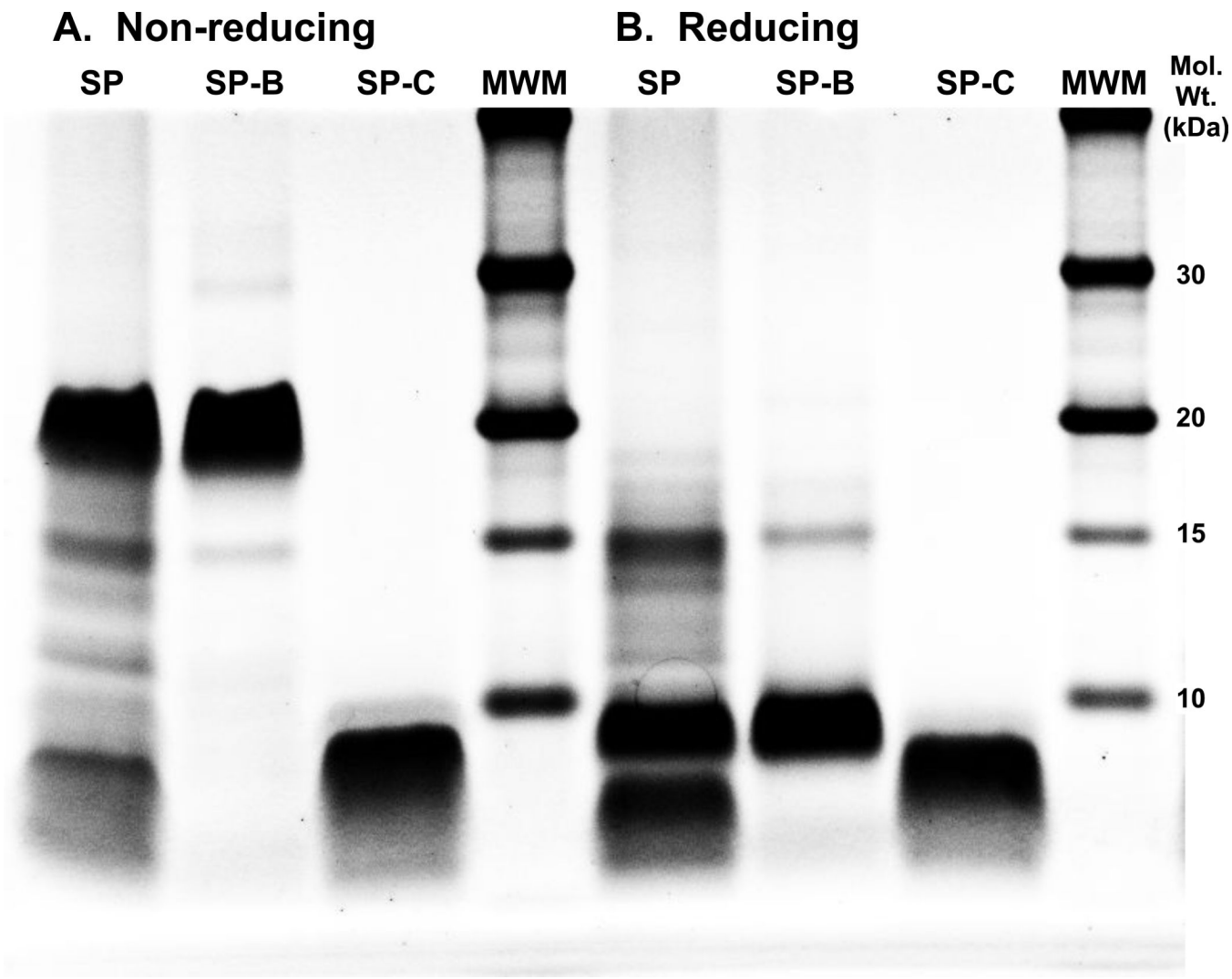

Figure 2.

Electrophoretic separation of the hydrophobic surfactant proteins. Labels indicate lanes containing the following samples: the combined proteins collected together from CLSE by gel permeation chromatography on a matrix of LH-20 (SP); SP–B separated from the SP by licensed use of a patented extraction procedure[37, 38] (SP–B); SP–C purified by extraction of the combined proteins followed by gel permeation chromatography on LH-60 (SP–C); molecular-weight markers (MWM) with the indicated molecular weights (Mol. Wt.). A. Non-reducing lanes: samples without dithiothreitol. B. Reducing lanes: samples containing 50 mM dithiothreitol.

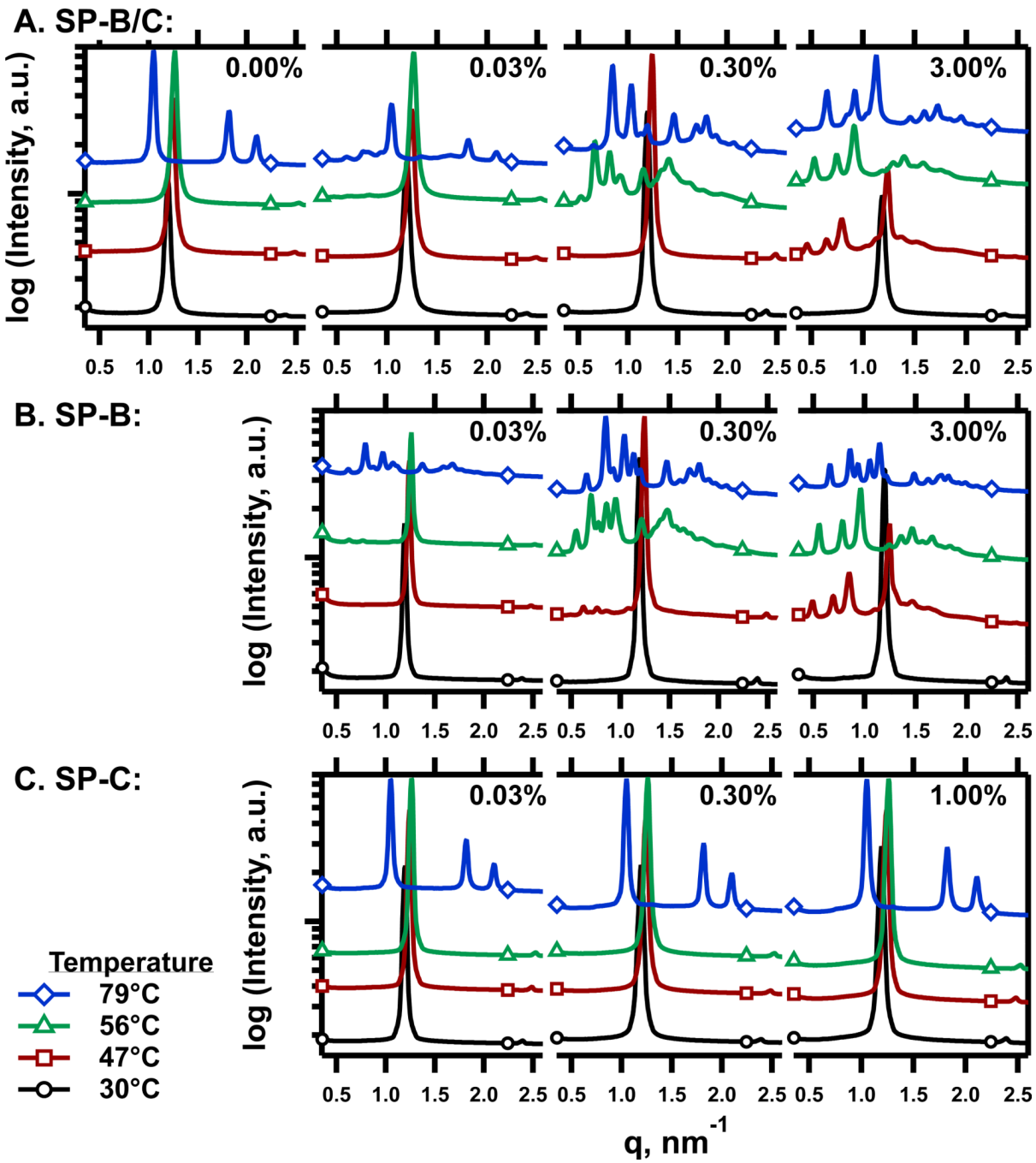

Figure 3.

Diffraction from POPE with the different surfactant proteins at different temperatures. Samples, dispersed in 2 mM EDTA, contained POPE with: A. the copurified hydrophobic proteins; B. SP–B; C. SP–C. Labels in each panel indicate the amount of protein (%, w:w) per phospholipid. The graph omits data at additional temperatures and amounts of protein for clarity of presentation.

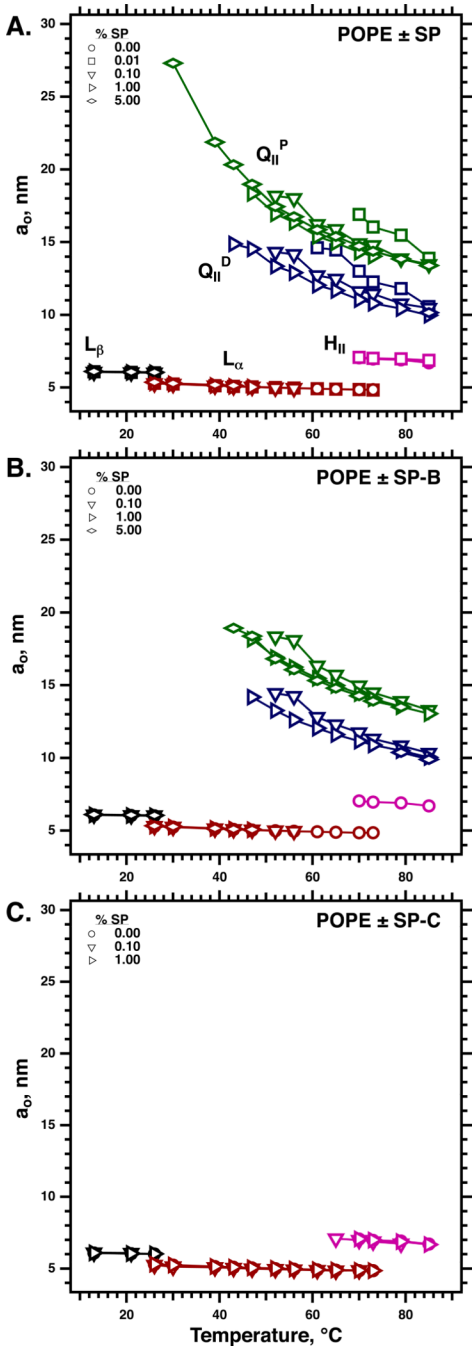

Figure 4.

Lattice-constant (a_o) of structures with the different space groups at different temperatures. Q_{II}^P and Q_{II}^D indicate bicontinuous cubic phases corresponding to the primitive (space group $Im\bar{3}m$) and diamond ($Pn\bar{3}m$) infinitely periodic minimal surfaces, respectively. POPE with: A. the copurified SP–B/C; B. SP–B; C. SP–C. Data from samples with 0.03, 0.30, and 3.00% protein are omitted for clarity of presentation.

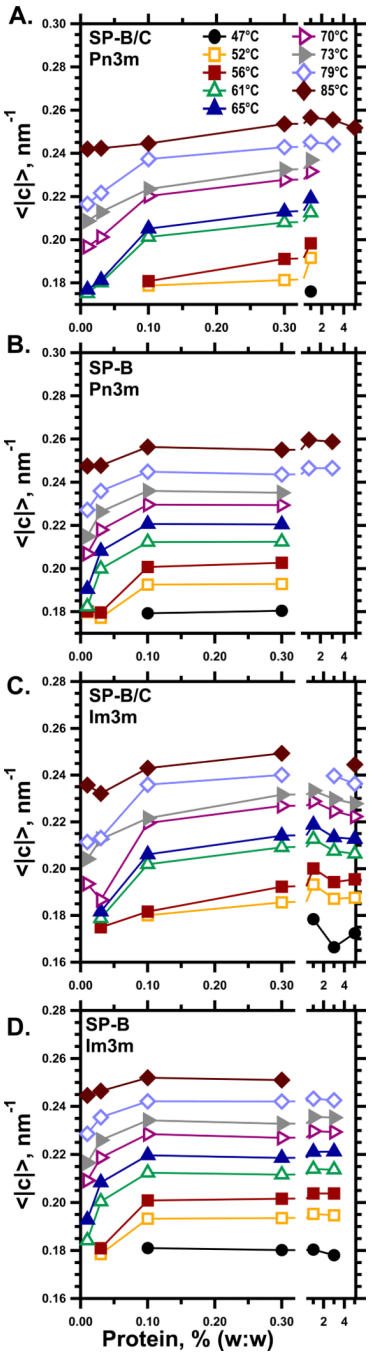

Figure 5.

Dose-response of the average curvature, <|c|>, for the Q_{II} phases to variable amounts of the combined proteins and SP–B. Panels indicate the average magnitude of the principal curvatures for the bilayer, given by the root of the average Gaussian curvature, $<|K|>^{1/2}$, of structures with $Pn\bar{3}m$ or $Im\bar{3}m$ space groups for POPE mixed with either the combined proteins or SP–B. The graphs omit results at 30–43°C because the range of protein concentrations that produced the Q_{II} phases at those temperatures was limited.